






Article

In Silico Identification and Experimental Validation of (–)-Muqubilin A, a Marine Norterpene Peroxide, as PPAR α / γ -RXR α Agonist and RAR α Positive Allosteric Modulator

Enrico D’Aniello ^{1,2}, Fabio Arturo Iannotti ^{2,3} , Lauren G. Falkenberg ⁴, Andrea Martella ³, Alessandra Gentile ³, Fabrizia De Maio ³, Maria Letizia Ciavatta ³, Margherita Gavagnin ³, Joshua S. Waxman ⁴ , Vincenzo Di Marzo ^{2,3,5} , Pietro Amodeo ^{3,*}  and Rosa Maria Vitale ^{3,*} 

¹ Department of Biology and Evolution of Marine Organisms, Stazione Zoologica “Anton Dohrn”, 80121 Naples, Italy; enrico.daniello@szn.it

² Endocannabinoid Research Group (ERG), Institute of Biomolecular Chemistry, National Research Council (ICB-CNR), Via Campi Flegrei 34, 80078 Pozzuoli (NA), Italy; fabio.iannotti@icb.cnr.it (F.A.I.); vdimarzo@icb.cnr.it (V.D.M.)

³ Institute of Biomolecular Chemistry, National Research Council (ICB-CNR), Via Campi Flegrei 34, 80078 Pozzuoli (NA), Italy; a.martella@lacdr.leidenuniv.nl (A.M.); alessandra.gentile@mpi-bn.mpg.de (A.G.); fabriziademaio@yahoo.it (F.D.M.); lciavatta@icb.cnr.it (M.L.C.); mgavagnin@icb.cnr.it (M.G.)

⁴ Molecular Cardiovascular Biology Division, Cincinnati Children’s Hospital Medical Center, Cincinnati, OH 45229, USA; lauren.falkenberg@cchmc.org (L.G.F.); Joshua.Waxman@cchmc.org (J.S.W.)

⁵ Canada Excellence Research Chair on the Microbiome-Endocannabinoidome Axis in Metabolic Health (CERC-MEND)-Université Laval, Quebec, QC G1V 0A6, Canada

* Correspondence: pamodeo@icb.cnr.it (P.A.); rmvitale@icb.cnr.it (R.M.V.)

Received: 16 January 2019; Accepted: 7 February 2019; Published: 12 February 2019



Abstract: The nuclear receptors (NRs) RAR α , RXR α , PPAR α , and PPAR γ represent promising pharmacological targets for the treatment of neurodegenerative diseases. In the search for molecules able to simultaneously target all the above-mentioned NRs, we screened an in-house developed molecular database using a ligand-based approach, identifying (–)-Muqubilin (Muq), a cyclic peroxide norterpene from a marine sponge, as a potential hit. The ability of this compound to stably and effectively bind these NRs was assessed by molecular docking and molecular dynamics simulations. Muq recapitulated all the main interactions of a canonical full agonist for RXR α and both PPAR α and PPAR γ , whereas the binding mode toward RAR α showed peculiar features potentially impairing its activity as full agonist. Luciferase assays confirmed that Muq acts as a full agonist for RXR α , PPAR α , and PPAR γ with an activity in the low- to sub-micromolar range. On the other hand, in the case of RAR, a very weak agonist activity was observed in the micromolar range. Quite surprisingly, we found that Muq is a positive allosteric modulator for RAR α , as both luciferase assays and in vivo analysis using a zebrafish transgenic retinoic acid (RA) reporter line showed that co-administration of Muq with RA produced a potent synergistic enhancement of RAR α activation and RA signaling.

Keywords: virtual screening; nuclear receptor agonist; positive allosteric modulator; zebrafish models

1. Introduction

Retinoic acid receptors (RARs), retinoid X receptors (RXRs) and peroxisome proliferator-activated receptors (PPARs) belong to the nuclear receptor (NR) family of ligand-activated transcription factors that regulate the expression of genes responsible for several physiological processes including cell

growth, differentiation, homeostasis, and apoptosis [1,2]. In mammals, there are three isotypes of each of these NRs, namely, α , β , and γ , which have high sequence homology and different tissue distributions [3,4]. NR family members share a common structural organization comprising an amino-terminal domain (A/B region), a central DNA binding domain (DBD), and a carboxy-terminal ligand-binding domain (LBD). In the absence of ligands, NRs act as transcriptional repressors by inhibiting the expression of downstream target genes. This mechanism is mediated by an interaction with an NR corepressor (NCoR) or the silencing mediator of retinoic acid thyroid hormone receptors (SMRT; also known as NCoR2) together with histone deacetylase 3 (HDAC3) [2]. Ligand binding to the LBD triggers the dissociation of corepressors and the formation of coactivator complexes by altering the conformation of a short helix, termed AF2, in the LBD and the recruitment of specific co-activators such as p300 and members of the steroid receptor coactivator (SRC) subfamily [5]. Once activated by their agonists, the resulting functional hetero- or homodimers bind to the response elements of their target genes, thus initiating transcription. RXRs form functional heterodimers with both RARs and PPARs, but may also form homodimers [1]. PPAR-RXR heterodimers are considered to be “permissive”, meaning that the heterodimers can be activated by either a PPAR or an RXR agonist and, when simultaneously activated, the heterodimer can respond in an additive or synergistic manner [1]. In contrast, RAR-RXR heterodimers are “conditionally permissive”, indicating that they are not activated by RXR ligands alone. Instead, it is the binding of an RAR agonist that initially activates the heterodimers and subsequently allows the binding of RXR ligands to enhance their transcriptional potential [6]. RAR and RXR ligands, referred to as retinoids and rexinoids, respectively, have been used to treat skin disorders and emphysema, as well as in cancer therapies [7]. Moreover, RXR α agonists can reduce fasting plasma glucose and counteract insulin resistance [8], and acting synergistically with PPAR γ agonists, are able to improve insulin-sensitivity [9]. Recently, it has also been shown that the stimulation of RAR α , RXR α , and PPAR α/γ may be beneficial in treating neurodegenerative diseases. In fact, studies carried out with experimental models of Alzheimer’s disease (AD) showed that the treatment with agonists of these NRs improved cognition and memory, improving disease-related pathology. Specifically, RXR agonists can stimulate the physiological clearance of amyloid- β (A β) [10], whereas PPAR γ agonists suppress the A β -mediated activation of microglia in vitro and prevent neural cell death [11,12] and PPAR α agonists can reduce endogenous A β production by inducing the α -secretase-mediated proteolysis of amyloid precursor protein (APP) [13]. Furthermore, it was found that dietary deficiency of vitamin A disrupts the retinoid signaling pathway in adult rats, leading to the deposition of amyloid- β in the cerebral blood vessels via down-regulation of RAR α in forebrain neurons and the loss of choline acetyltransferase (ChAT) expression [14,15]. These changes were reversed by the administration of retinoic acid (RA). Moreover, histological samples from AD patients showed a deficit of RAR α expression and a deposition of A β in the surviving neurons [14]. Altogether, the ability of RAR and PPAR stimulation to affect A β accumulation suggests that compounds with broad agonist activity toward RAR α , RXR α , and PPAR α and $-\gamma$ could represent useful pharmacological tools to provide novel inroads for the treatment of neurodegenerative diseases.

Natural compounds represent an invaluable source of bioactive compounds potentially able to act on multiple-related targets due to their versatile scaffolds and functional groups. By continuing our search for multiligand agents from natural sources [16–18], we focused our attention in this work on compounds potentially able to bind and activate nuclear receptors such as RXR α , RAR α , and PPAR α/γ , because they may have therapeutical potential for the treatment of neurological diseases such as Alzheimer’s disease. With this aim, we used a ligand-based approach [19] to screen and identify possible candidates in our in house-developed database StOrMoDB (Structurally Oriented Molecular DataBase) of marine natural compounds and found (–)-Muqubilin A (Muq) as a potential hit. Muq is a norterpene cyclic peroxide described from distinct Red Sea sponges [20,21] and recently isolated in our institute from the sponge *Diacarnus erythraeanus* [22]. Norterpene cyclic peroxides are active metabolites endowed with cytotoxic activity against a variety of cancer cell lines [21–24]. The ability

of this compound to act as a potential multiligand agent for RAR α -RXR α -PPAR α/γ was assessed by molecular docking and molecular dynamics simulations and then validated by luciferase assays. While Muq was found to act as a full agonist of RXR α , PPAR α , and PPAR γ , and as a weak agonist for RAR α , luciferase and in vivo transgenic reporters in zebrafish showed that it is also a positive allosteric modulator of RAR α . Therefore, our results indicated that the marine compound Muq is endowed with a broad agonist activity for multiple NRs, which may suggest its potential use against neurodegenerative diseases.

2. Results

2.1. Virtual Screening of Our In-House Molecular Database

A ligand-based virtual screening (VS) approach was used to identify possible RXR α , RAR α , and PPAR α/γ multiligands in our in-house developed database StOrMoDB, which contains 350 compounds of marine origin, isolated and characterized at the Institute of Biomolecular Chemistry, National Research Council (ICB-CNR), for which samples are currently available for experimental validation. The VS was performed by running DB queries based on SMARTS strings (see Section 4.1, “Computational Methods”) encoding the RA-derived scaffold that we hypothesized to provide multiligand properties against the selected targets. This scaffold featured a 2,6,6-trimethylcyclohexen-1-yl ring (TMCH), that is, the pendant group of RA, and a carboxylate group, separated by a proper spacer producing an elongated structure, which can ensure a favorable ligand accommodation in the LBD of both retinoids and PPAR proteins. The search produced a norterpene cyclic peroxide (–)-Muqubilin A, here termed Muq, as a positive hit (Figure 1). Muq was then subjected to molecular docking and molecular dynamics (MD), as described in the experimental section, to assess the propensity of the molecule to effectively bind the above-mentioned molecular targets.

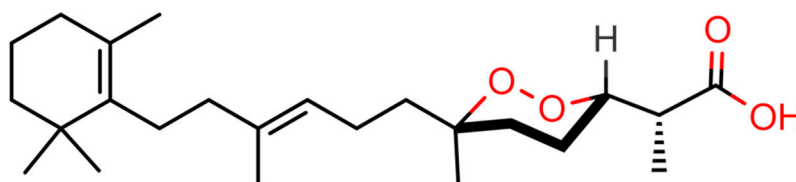


Figure 1. Chemical structure of (–)-Muqubilin (Muq) A. Heteroatoms and polar hydrogens are colored red.

2.2. Muq-RXR α Complex Model

The best docking pose of Muq into RXR α underwent 50 ns of MD to assess its stability. Analysis of the MD trajectory (Figure S2, Supplementary Materials) shows that Muq adopts a very stable pose within the LBD, preserving an arrangement similar to the starting docking pose. Figure 2A illustrates the last MD frame as representative of this complex. The molecule is hosted in the hydrophobic pocket formed by residues lying on helices H3, H5, H7, and H11 and on the β -turn. The carboxylate group is involved in three H-bond interactions, a polar network also found in the experimental *cis*-retinoic acid-RXR α complex structure (PDB ID: 1FBY): one reinforced by ionic interaction with Arg316(H5) (MD occurrence >90%), and the others with Gln275(H3) side-chain (MD occurrence >55%) and with the amide backbone of Ala327(β -turn) (MD occurrence >58%). The cyclic peroxide is sandwiched between Phe313(H5) and Ala 272(H3), whereas the cyclohexenyl ring is hosted in the hydrophobic pocket formed by helices H7 and H11, which is the same site docking the TMCH group in the experimental *cis*-retinoic acid-RXR α complex structure. The overall arrangement of Muq in the LBD and the network of polar interactions engaged by the molecule is strongly suggestive of a full agonism behavior on RXR α .

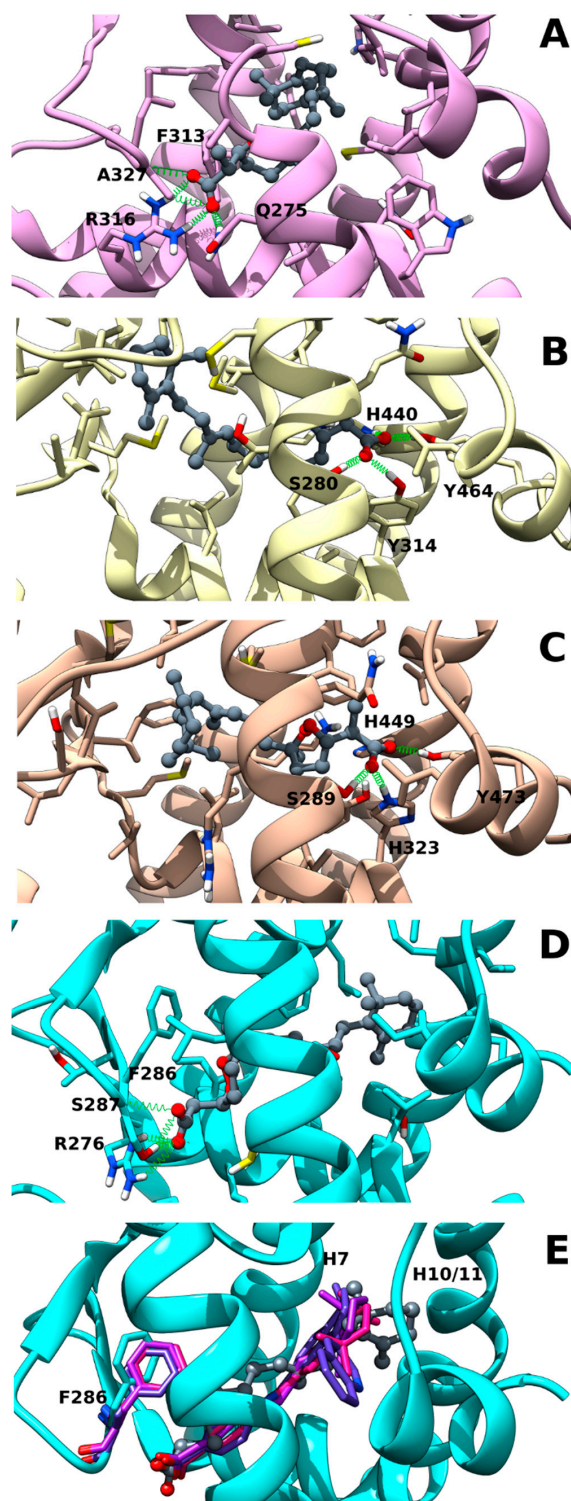


Figure 2. Representative frames from molecular dynamics (MD) of Muq-nuclear receptor (NR) complexes. (A) Muq-RXR α ; (B) Muq-PPAR α ; (C) Muq-PPAR γ ; (D) Muq-RAR α ; (E) best fit between Muq-RAR α MD frame (protein and Muq shown) and experimental structures of RAR α in complex with agonists (only ligands shown: PDB ID: 3KMR, magenta; 3A9E, purple; 1DKF, blue). Ball and stick and stick-only representations are used for ligand heavy atoms and protein sidechain atoms within 5 Å from ligand, respectively. Carbon atoms are painted according to ribbons for proteins and dark gray for Muq, Hydrogen, nitrogen, oxygen, and sulfur atoms are painted white, blue, red, and yellow, respectively. A “green spring” representation is adopted for H-bonds involving ligand atoms.

2.3. Muq-PPAR α / γ Complex Models

The same computational protocol adopted for RXR α was also applied to PPAR α and PPAR γ molecular targets. The resulting complexes show that Muq is well accommodated in the LBD of both PPARs, giving rise to stable complexes, which exhibit neither significant drift throughout the whole MD simulations nor appreciable deviations from their starting docking poses. However, the formation of interactions with residues lying on the Ω -loop during MD induces a more extended ligand conformation in the PPAR α -Muq complex in comparison with the starting docking pose. On the other hand, the Muq pose in the PPAR γ complex, even if characterized by a higher flexibility in comparison to PPAR α (see Figure S2, Supplementary Materials), preserves in MD the same overall arrangement of the starting docking pose. The last frames of each complex, taken as representative of the corresponding trajectories, are shown in Figure 2B,C. Muq adopts a horseshoe conformation embracing helix H3 in both PPAR binding sites, orienting its carboxyl group toward H12 and the cyclohexenyl ring toward the β -sheet and the Ω loop. The carboxyl group engages a network of stable H-bond interactions with PPAR α -Tyr464 (MD occurrence >60%)/PPAR γ -Tyr473(H12) (MD occurrence >90%), PPAR α -His440 (MD occurrence >55%)/PPAR γ -His449(H10/11) (MD occurrence >38%), PPAR α -Tyr314 (MD occurrence >80%)/PPAR γ -His323(H5) (MD occurrence >55%), and PPAR α -Ser280 (MD occurrence >11%)/PPAR γ -Ser289(H3) (MD occurrence >21%). Since Muq exhibits overall arrangements in both PPAR isoforms that recapitulate those of classical PPAR α / γ full agonists, it is expected to act as a dual PPAR α / γ agonist.

2.4. Muq-RAR α Complex Model

The *in silico* screening was also used to evaluate the potential ability of Muq to bind RAR α . As with the other NRs, Muq is able to accommodate well into the LBD, adopting a binding stable pose during the whole MD simulation, even if characterized by higher flexibility than in the RXR α complex (see Figure S2, Supplementary Materials) The last frame from MD was taken as representative and is shown in Figure 2D. Ligand-protein H-bonds are formed between the Muq carboxylate group and both Ser287(β -turn) backbone/sidechain (MD occurrence >50% and 90%, respectively) and Arg276 (H5) sidechain (MD occurrence >75%), this latter reinforced by ionic interactions. This polar network is common to known agonists in their experimental structures of RAR α complexes (PDB ID: 3KMR, 3A9E, and 1DKF). However, the overall arrangement of Muq in the RAR α LBD shows peculiar features since the methyl on the peroxide ring induces a rotation of Phe286(β -turn) sidechain and the cyclohexenyl ring occupies a larger fraction of cavity between helices H7 and H10/11 in comparison with other agonists in their crystallographic complexes with RAR α (Figure 2E). These features could in principle negatively affect the ability of Muq to act as a full agonist for this NR.

2.5. Muq is an Agonist for RXR α and PPAR α / γ

To confirm the computational predictions of Muq binding to RXR α receptors, we transfected COS-7 cells with human chimeric RXR α -LBD-Gal4 constructs together with the TK-MH100x4 construct, which contain four direct tandem copies of the UAS (upstream activating sequence) enhancer. These types of fusion proteins have been used to assess the functions of individual NR domains [25]. The day after plating, cells were treated with the RXR agonist 9-*cis*-retinoic acid and Muq at 0.1, 1, and 10 μ M. Higher concentrations were not investigated since in a separate set of experiments, COS-7 cell viability measured by MTT assays was significantly reduced (see Figure S1, Supplementary Materials), in agreement with a previous study reporting a reduction of viability with a mean IC₅₀ of 17 \pm 7 μ M and 9 \pm 2 μ M in normal (fibroblasts, epithelial cells, and keratinocytes) and cancer cell lines, respectively [22].

Results in Figure 3A clearly show that *in vitro* Muq is able to activate the *h*RXR α fusion protein as a full agonist in a concentration–response manner, in agreement with the computational data, with a 10 μ M concentration promoting a >300-fold increase in measured activation. Thus, Muq can function as a strong agonist for *h*RXR α . Given these results, we posit that the activity of Muq as a potent RXR agonist could also

explain the greater cytotoxicity exhibited by this molecule toward the cancer cell lines in comparison with the normal ones [22], since RXR agonists are known to act as effective chemotherapeutic agents [26,27].

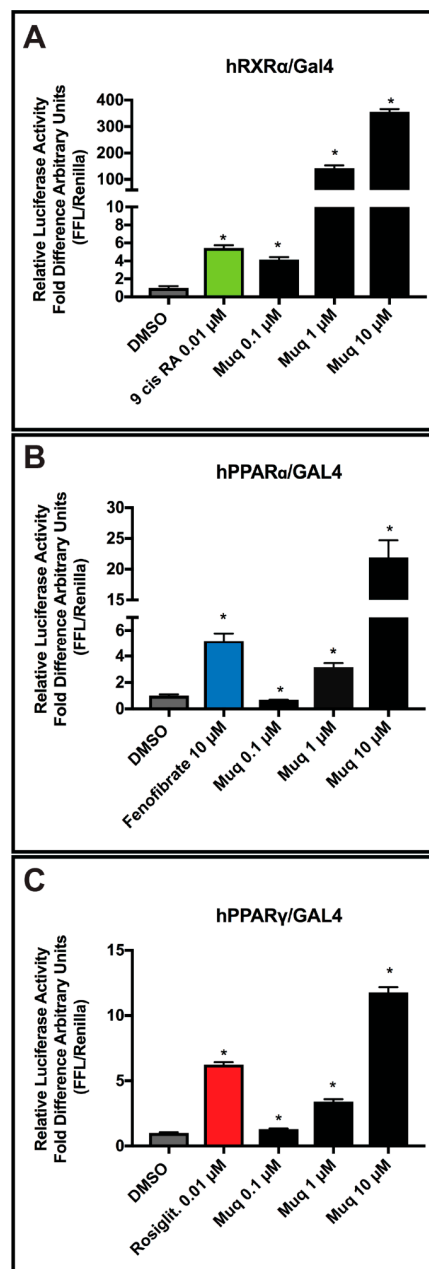


Figure 3. Luciferase assays. (A) Muq acts as an agonist on hRXRα-LBD. Relative luciferase activity in response to 0.1, 1, and 10 μM of Muq. 9-*cis*-retinoic acid at 0.01 μM was used as an RXRα agonist positive control. (B) Muq acts as an agonist on hPPARα-LBD. Relative luciferase units in response to 0.1, 1, and 10 μM of Muq. Fenofibrate at 10 μM was used as an hPPARα agonist positive control. (C) Muq acts as an agonist on hPPARγ-LBD. Relative luciferase units in response to 0.1, 1, and 10 μM of Muq. Rosiglitazone at 0.01 μM was used as an hPPARγ agonist positive control. The activity of the vehicle control was set at 1 and the relative luciferase activity obtained for each control and concentrations tested are presented as a fold induction with respect to the vehicle control. Statistical analysis was performed by comparing each concentration of Muq and of the specific agonist to the vehicle control using the Student's *t*-test. The analyses were performed using GraphPad Prism 7 software. Statistically significant differences were accepted when the *p*-value was at least ≤ 0.05 . Data are expressed as means \pm SEM, (*n* = 3). * *p* ≤ 0.05 .

Next, we examined if Muq was able to function as an agonist for *hPPAR* α/γ receptors as predicted by our computational study. As with the *hRXR* α -LBD-Gal4 fusion, the ability of Muq to activate these receptors was assayed using chimeric *hPPAR* α -LBD-Gal4 and *hPPAR* γ -LBD-Gal4 constructs transfected together with a UAS enhancer. As shown in Figure 3B,C, Muq was able to induce transcriptional activation of both PPAR-Gal4 chimeras, but produced a greater activation by *hPPAR* α than the *hPPAR* γ fusion. Overall, our in vitro data confirm the full agonist ability of Muq for both *hPPAR* α and *hPPAR* γ receptors.

2.6. Muq Functions as an Allosteric Enhancer of RA on *hRAR* α

While our computational results suggested a canonical agonist behavior for Muq on *RXR* α and *PPAR* α/γ , the results for *RAR* α , although still supporting an appreciable interaction with the receptor, showed a significant deviation from structural requirements for canonical agonism. By using *hRAR* α -LBD-Gal4 fusion proteins, again equivalent to those assayed for the other NRs, we found that Muq weakly stimulated *hRAR* α -LBD-Gal4 proteins compared to RA in the reporter assay (Figure 4A). However, unexpectedly, we found that the co-administration of RA with Muq showed a synergistic enhancement of reporter activation that cannot be ascribed to the agonistic effect of Muq on *RXR* α , since the Gal4-fusion construct should function independently from *RXR* α . Given these surprising results obtained analyzing the *hRAR* α -LDB fusion, we sought to confirm the synergistic effect of Muq with RA by carrying out additional in vitro and in vivo experiments. We chose zebrafish embryos due to the accessibility of available tools to assess RAR function and RA signaling in these animals [28]. Moreover, RARs are highly conserved proteins in vertebrates [29], with the LBD of zebrafish *RAR* $\alpha\alpha/b$ sharing >90% sequence identity with the LBD of *hRAR* α . We first performed the UAS luciferase reporter assays using a zebrafish *RAR* $\alpha\beta$ -LBD-Gal4 chimeric construct [30]. We obtained similar results in comparison with the *hRAR* α -LBD-Gal4 fusion, again observing a weak activation alone and a potentiating effect of Muq with RA (Figure 4B). Together, the in vitro analysis strongly suggests the presence of an additional, positive allosteric site for Muq, since the orthosteric one would not allow the simultaneous binding of both Muq and RA.

Finally, we wanted to determine if Muq was able to act as enhancer of RA also in vivo. Therefore, we treated zebrafish embryos carrying the RA signaling reporter line *Tg(12XRARE-elf1a:EGFP)^{sk72}* [31] from 24 hpf until 48 hpf with 0.5 μ M RA and 10 μ M Muq alone and together, and then we analyzed the morphology of the embryos and the expression of GFP. A 0.5 μ M portion of RA was used, in contrast to 0.001 μ M RA from the in vitro reporters, because this produces a perceptible, yet minimal upregulation of GFP in vivo (Figure 4F). While 10 μ M Muq did not produce a perceptible effect on the embryos compared to the DMSO (control) treatment (Figure 4F), the combination of RA and Muq enhanced both the teratogenic morphological defects (smaller heads and shortened tails [28,29]) and the GFP expression of the RA reporter compared to RA treatment alone (Figure 4I,J). Therefore, our in vivo analysis of Muq with RA in zebrafish embryos recapitulates the same trends observed in the in vitro assays using chimeric humans and zebrafish *RAR* α .

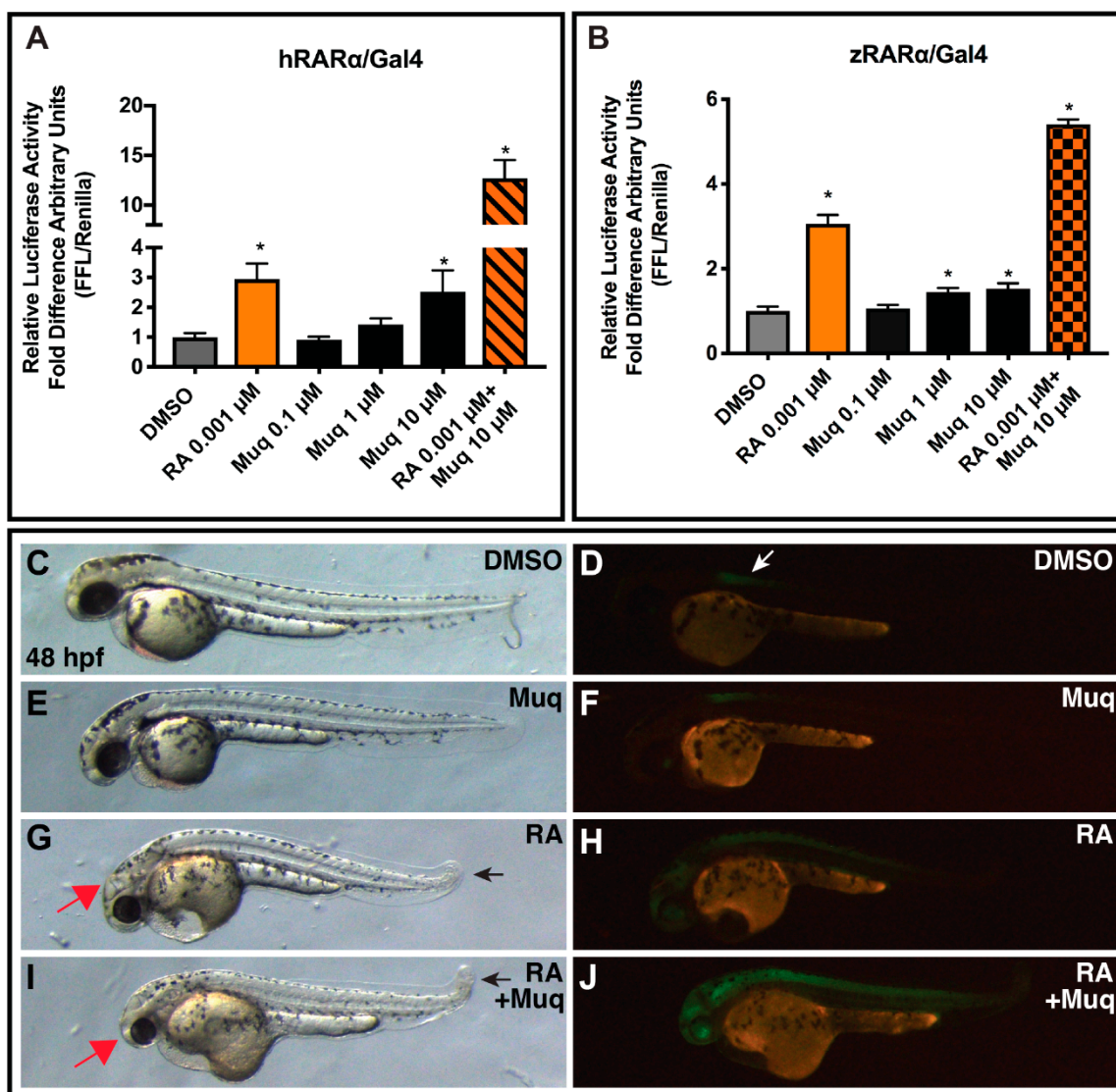


Figure 4. Muq synergistically reinforces (A) human RAR α in vitro and (B) zebrafish RAR α in vitro. Relative luciferase units in response to 0.1, 1, and 10 μ M of Muq. Retinoic acid (RA) at 0.001 μ M was used as an *hRAR* α and a *zRAR* α agonist positive control. The activity of the vehicle control was set at 1 and the relative luciferase activities obtained for each control and concentration tested are presented as a fold induction with respect to the vehicle control. Statistical analysis was performed by comparing each concentration of Muq and that of RA to the vehicle control using the Student's *t*-test. The analyses were performed using GraphPad Prism 7 software. Statistically significant differences were accepted when the *p*-value was at least ≤ 0.05 . Data are expressed as means \pm SEM, (*n* = 9) for human RAR α and (*n* = 3) for zebrafish RAR α . * *p* ≤ 0.05 . (C) Muq behaves as a weak RAR α agonist and enhances RA signaling in zebrafish. Embryos carrying the *12XRARE-ef1a:EGFP* transgene at 48 hpf that were treated from 24 hpf with (C,D) DMSO, (E,F) 10 μ M Muq, (G,H) 0.5 μ M RA, and (I,J) 0.5 μ M RA + 10 μ M Muq. Embryos in C, E, G, and I are the same as D, F, H, and J. Red arrows in G and I indicate smaller eyes. Black arrows in G and I indicate shortened tail. White arrow indicates E-GFP from the transgene in the anterior spinal cord. For this study, 25 embryos per condition were examined.

3. Discussion and Conclusions

The norterpene cyclic peroxide Muq emerging from the search in our in house-developed database StOrMoDB was subjected to molecular docking and molecular dynamics simulations to assess its ability to actually bind the aforementioned NRs. In fact, this class of molecules has been previously

reported as cytotoxic [21,22] and/or antimalarial agents [32], but not as NR ligands. The binding modes found for Muq in the LBD of RXR α , PPAR α , and PPAR γ were compatible with a full agonism, since both the pattern of the polar interactions and the orientation of the hydrophobic tail recapitulated the binding mode of canonical agonists. In fact, full PPAR agonists adopt a horse-shoe conformation in the LBD, engaging H-bonds with Ser(H3)/His(H10/119) and Tyr(H12), and hydrophobic interactions with residues lying on the β -sheet, whereas RXR agonists engage H-bonds involving Arg316(H5) sidechain and Ala (β -turn) backbone with the hydrophobic pendant lying between helices H7 and H10/11. On the other hand, for RAR α LBD, the binding mode of Muq showed some peculiar features in comparison with other experimentally solved complexes with agonists, potentially impairing the ability of this compound to act as a canonical agonist. In particular, the TMCH group of Muq occupies a larger volume of the pocket between helices H7 and H10/11, and the cyclic peroxide group induces a rotation of the β -turn Phe286 sidechain, whose orientation is well conserved in the experimental complexes. The subsequent validation of the computational results by luciferase assays confirmed that Muq is a potent *h*RXR α agonist and a full agonist for *h*PPAR α/γ , whereas it is a only a weak agonist for *h*RAR α . Thus, the peculiar features observed in the binding mode of Muq into the RAR α LBD negatively affected its ability to directly activate this NR. However, since MD predicted a stable binding for the Muq-RAR α complex, we also evaluated the ability of Muq to modulate the effect of RA. The co-administration of Muq and RA showed a strong additive effect, which can be neither ascribed to the effects of Muq on *h*RXR α , since the Gal4 construct was used in luciferase assays, nor predicted from the modelled structure of the Muq-RAR α complex shown in Figure 2E, which would not allow the coexistence of Muq and RA in the LBD site. This interesting finding was confirmed by both luciferase assays on zebrafish RXR α LBD and morphological and GFP-expression studies on zebrafish embryos, disclosing an effect of Muq as positive allosteric modulator for this NR.

In conclusion, using a combination of computational and experimental approaches, we have identified Muq as a novel multiligand exerting full agonist activity at RXR α and PPAR α/γ receptors and positive allosteric modulatory activity at RAR α . Importantly, our results propose Muq as a candidate in the treatment of neurodegenerative diseases, such as Alzheimer's disease, where a broad stimulation of this NR pool could provide greater benefits than pharmacological approaches targeting each NR individually. Moreover, the potent agonism of Muq at RXR α could also explain the previously reported cytotoxic activity exhibited against different cancer cell lines [22]. To the best of our knowledge, Muq represents the first example of a positive allosteric modulator of RAR α . Although further studies are required to identify the allosteric binding site of RAR α , and to assess the activity of Muq in experimental models of disease, we envision that our results could pave the way to a deeper understanding of the mechanisms regulating NR function and to the discovery of new pharmacological tools to treat neurological diseases and cancers.

4. Materials and Methods

4.1. Computational Methods

Virtual screening of the StOrMoDB database (<https://stormodb.na.icb.cnr.it/stormodb>) was performed using the featured SMARTS pattern querying option on DB compounds for which samples for experimental validation were eventually available (350 molecules, all of marine origin). To search for molecules featuring a 2,6,6-trimethylcyclohexen-1-yl ring (TMCH) separated from a carboxylate group by a variable-length spacer, the general SMARTS pattern CC1(C)CCCC(C)=C1C-,-,#,@{[*]-,-,#,@}n[C,c](=[O,o])[OH,oH,O-,o-] (where "{[*]-,-,#,@}n" stands for "n repeats of the [*]-,-,#,@ pattern") was used in fourteen queries in which the spacer length n was allowed to vary from 3 to 16. The only hit, Muq, was obtained for n = 10.

Starting ligand geometry was built with Ghemical 2.99.2 [33] followed by energy minimization (EM) at molecular mechanics level first, using Tripos 5.2 force field parametrization [34], and then at AM1 semi-empirical level; fully optimized using GAMESS program [35] at the Hartree-Fock level with

STO-3G basis set; and subjected to HF/6-31G*/STO-3G single-point calculations to derive the partial atomic charges by the RESP (Restrained ElectroStatic Potential) procedure [36]. Docking studies were performed with AutoDock Vina1.1.2 [37], by using the crystallographic structures of RXR α , RAR α , PPAR α , and PPAR γ (PDB:3R5M, 3KMR, 2P54, and 2F4B, respectively). Both proteins and ligands were processed with the AutoDock Tools (ADT) package version 1.5.6rc1 [38] to merge non polar hydrogens, calculate Gasteiger charges, and select the rotatable side-chain bonds. Grids for docking evaluation were generated using the program AutoGrid 4.2 included in AutoDock 4.2 distribution, setting a spacing of 0.375 Å and a resolution of 60 × 60 × 60 points for PPAR γ and RXR α , 50 × 50 × 70 points for PPAR α , and 60 × 60 × 70 points for RAR α , centered on the ligand-binding site, by positioning the center of the grid in proximity of Tyr327 for PPAR γ , Ser280 for PPAR α , Cys432 for RXR α , and Leu269 for RAR α . The following parameters were used for AutoDock Vina: exhaustiveness of 8, energy threshold of 10 kcal mol⁻¹, and up to 100 poses for each compound (Vina automatically only reports “interesting” poses within the energy threshold, which, for the selected input parameters, produced 20 poses per run for all the docking runs with the exception of those for the X-ray ligands of PPARs, which were four for PPAR α and two for PPAR γ). For each simulated complex, the pose exhibiting the most favorable Vina binding energy value was selected as the representative binding pose from docking. For comparison purposes, reference compounds were used in docking calculations: RA for both RXR α and RAR α and the corresponding X-ray ligands for PPAR α and PPAR γ . The energy values for the best-scoring poses between Muq and the reference compounds were comparable. In detail, we obtained values of -10.0 (RA) vs. -8.2 kcal mol⁻¹ (Muq) for RXR α , -9.1 (RA) vs. -10.0 kcal mol⁻¹ (Muq) for RAR α , -6.9 (GW735) vs. -6.8 kcal mol⁻¹ (Muq) for PPAR α , and -12.6 ((5-[3-[(6-benzoyl-1-propyl-2-naphthyl)oxy]propoxy]-1H-indol-1-yl) acetic acid) and -8.2 (Muq) kcal mol⁻¹ for PPAR γ . The selected complexes were then completed by the addition of all hydrogen atoms and underwent EM and then MD simulations with Amber16 pmemd.cuda module [39], using the ff14SB version of AMBER force field for the protein and gaff parameters [40] for the ligand.

To perform MD simulations in solvent, the complexes were confined in TIP3P water periodic truncated octahedron boxes exhibiting a minimum distance between solute atoms and box surfaces of 10 Å, using the tleap module of the AmberTools16 package. The systems were then neutralized by the addition of counterions (Na⁺) and subjected to 1000 steps of EM with solute atoms harmonically restrained to their starting positions ($K_r = 10$ kcal mol⁻¹ Å⁻¹). Then, 90 ps restrained MD ($K_r = 5$ kcal mol⁻¹ Å⁻¹) at constant volume was run on each solvated complex, gradually heating the system to 300 K, followed by 60 ps restrained MD ($K_r = 5$ kcal mol⁻¹ Å⁻¹) at constant temperature (300 K) and pressure (1 atm) to adjust system density. Production MD simulations were carried out at constant temperature (300 K) and pressure (1 atm) for 50–100 ns, with a time-step of 2 fs. Bonds involving hydrogens were constrained using the SHAKE algorithm [41]. The Cpptraj module of AmberTools16 and program UCSF Chimera 1.10.1 [42] were used to perform MD analysis and to draw the figures, respectively.

4.2. Purification of (-)-Muqubilin A

The amount of Muq used in tests was obtained from the lipophilic extract of the Red Sea sponge *Diacarnus erythraeanus*. Isolation, purification, and identification of Muq have been previously described [22].

4.3. Luciferase Assay

COS-7 cells (monkey kidney fibroblast-like cells) were grown in DMEM supplemented with 10% fetal bovine serum and 1% Pen/Strep under standard conditions. Cells were plated in 24-well dishes at 70% confluence and transfected using Lipofectamine LTX and PLUS Reagent (cat. 15338-100; Thermo Fisher Scientific, Milan IT) according to the manufacturer's instructions.

Briefly, at day 1, for each well, a combination of 25 ng of CMX-Gal4-*hRXR* α , or 25 ng of pM1-*hPPAR* α -Gal4, or pM1-*hPPAR* γ -Gal4, or pSG5-Gal4-*hRAR* α , or with zebrafish RAR α was transfected together with 300 ng of TK-MH100x4-Luc containing the UAS enhancer elements, 25 ng

of Renilla Luciferase (pRL, cat. E2231; Promega, Milan, Italy), and 150 ng pcDNA3 (Thermo Fisher Scientific, Milan, Italy) empty vector to obtain a total of 500 ng. The next day, the growth media was replaced with fresh media containing compounds of interest. The DMSO was used as vehicle. Fenofibrate (cat. F6020; Sigma-Aldrich), rosiglitazone (cat. 5325; Tocris, Bristol, UK), 9-*cis*-retinoic acid (cat. R4643; Sigma-Aldrich), and retinoic acid (cat. R2625; Sigma-Aldrich) were used respectively as agonist of PPAR α , PPAR γ , hRXR α , and human and zebrafish RAR α . On day 3, after 18 hours of treatment, the cells were harvested and processed for the luciferase and Renilla luciferase (Promega) using the Dual-Luciferase Reporter Assay System (Promega, cat. E1910) and detected using the GloMax Luminometer (Promega).

4.4. MTT Assay

COS-7 cells were grown in DMEM supplemented with 10% FBS, L-glutamine and 1% Pen/Strep under standard conditions in 48-well cell culture plates. After adhesion, cells were serum-deprived and treated with the desired concentrations of compounds for 18 h (the absence of serum was maintained during the treatments). Cell viability was assessed by the MTT assay following published procedures [43].

4.5. Zebrafish Husbandry and Treatments

All zebrafish husbandry and experiments were performed in accordance with protocols approved by the Institutional Animal Care and Use Committee (IACUC) of Cincinnati Children's Hospital Medical Center. The zebrafish transgenic line *Tg(12XRARE-elf1a:EGFP)^{sk72}* was used in experiments. Zebrafish embryo were treated with RA and/or Muq at the concentrations indicated above. Then, 25 embryos per condition were placed in glass vials with 2 mL of embryo water. RA from a 10⁻¹ M stock in DMSO was diluted 1:100 in DMSO followed by a subsequent dilution to the final concentration in fish water. Muq was diluted to the final concentration in embryo water from a 10⁻² M stock in DMSO. Embryos were placed on a nutator in an incubator for 24 hpf. Their morphology and fluorescence were examined and imaged using a Zeiss M2Bio_V8 (Carl Zeiss Microscopy, Thornwood, NY, USA) fluorescent microscope.

Supplementary Materials: The following are available online at <http://www.mdpi.com/1660-3397/17/2/110/s1>, Figure S1: Effect of Muqubilin on the viability of COS-7 cells, Figure S2: Evaluation of stability of the ligand binding mode during the last 30 ns of MD.

Author Contributions: Conceptualization, E.D.A., R.M.V., and P.A.; methodology, E.D.A., F.A.I., R.M.V., P.A., J.S.W., and V.D.M.; validation, E.D.A., F.A.I., R.M.V., P.A., and J.S.W.; formal analysis, E.D.A., F.A.I., A.G., and L.G.F., R.M.V., A.M., and F.D.; investigation, E.D.A., F.A.I., R.M.V., P.A., J.S.W., L.G.F., M.L.C., M.G., A.M., A.G., and V.D.M.; writing—original draft preparation, E.D.A. and R.M.V.; writing—review and editing, E.D.A., R.M.V., P.A., J.S.W., and V.D.M.; visualization, E.D.A., R.M.V., and P.A.

Acknowledgments: The authors are very grateful to Steven Kliewer from UTSW Medical Center (Dallas, Texas) for the kind gift of the CMX-Gal4-hRXR α and TK-MH100x4-Luc plasmids, Karsten Kristiansen, from the University of Copenhagen for the kind gift of pM1-hPPAR α -Gal4 and pM1-hPPAR γ -Gal4 plasmids, and Prof. Michael Privalsky from the University of California, Davis for the kind gift of pSG5-Gal4-hRAR α plasmid. Finally, the authors are deeply grateful to Marco Allarà for his help with the cell culture and Salvatore Donadio for programming and technical support on StOrMoDB.

Conflicts of Interest: The authors declare no conflict of interest.

References

- Huang, P.; Chandra, V.; Rastinejad, F. Retinoic acid actions through mammalian nuclear receptors. *Chem. Rev.* **2014**, *114*, 233–254. [[CrossRef](#)] [[PubMed](#)]
- Sever, R.; Glass, C.K. Signaling by nuclear receptors. *Cold Spring Harb. Perspect. Biol.* **2013**, *5*, a016709. [[CrossRef](#)] [[PubMed](#)]
- Berger, J.; Moller, D.E. The Mechanisms of Action of PPARs. *Annu. Rev. Med.* **2002**, *53*, 409–435. [[CrossRef](#)]
- Altucci, L.; Leibowitz, M.D.; Ogilvie, K.M.; de Lera, A.R.; Gronemeyer, H. RAR and RXR modulation in cancer and metabolic disease. *Nat. Rev. Drug Discov.* **2007**, *6*, 793–810. [[CrossRef](#)] [[PubMed](#)]

5. Glass, C.K.; Saijo, K. Nuclear receptor transrepression pathways that regulate inflammation in macrophages and T cells. *Nat. Rev. Immunol.* **2010**, *10*, 365–376. [[CrossRef](#)] [[PubMed](#)]
6. Moutinho, M.; Landreth, G.E. Therapeutic potential of nuclear receptor agonists in Alzheimer's disease. *J. Lipid Res.* **2017**, *58*, 1937–1949. [[CrossRef](#)]
7. Uray, I.P.; Dmitrovsky, E.; Brown, P.H. Retinoids and rexinoids in cancer prevention: From laboratory to clinic. *Semin. Oncol.* **2016**, *43*, 49–64. [[CrossRef](#)]
8. Zhang, H.; Xu, X.; Chen, L.; Chen, J.; Hu, L.; Jiang, H.; Shen, X. Molecular determinants of magnolol targeting both RXR α and PPAR γ . *PLoS ONE* **2011**, *6*, e28253. [[CrossRef](#)]
9. Bhatia, V.; Viswanathan, P. Insulin resistance and PPAR insulin sensitizers. *Curr. Opin. Investig. Drugs* **2006**, *7*, 891–897. [[PubMed](#)]
10. Cramer, P.E.; Cirrito, J.R.; Wesson, D.W.; Lee, C.Y.D.; Karlo, J.C.; Zinn, A.E.; Casali, B.T.; Restivo, J.L.; Goebel, W.D.; James, M.J.; et al. ApoE-Directed Therapeutics Rapidly Clear Amyloid and Reverse Deficits in AD Mouse Models. *Science* **2012**, *335*, 1503–1506. [[CrossRef](#)]
11. Heneka, M.T.; Reyes-Irisarri, E.; Hull, M.; Kummer, M.P. Impact and therapeutic potential of PPARs in Alzheimer's Disease. *Curr. Neuropharmacol.* **2011**, *9*, 643–650. [[CrossRef](#)] [[PubMed](#)]
12. Kim, E.J.; Kwon, K.J.; Park, J.Y.; Lee, S.H.; Moon, C.H.; Baik, E.J. Effects of peroxisome proliferator-activated receptor agonists on LPS-induced neuronal death in mixed cortical neurons: associated with iNOS and COX-2. *Brain Res.* **2002**, *941*, 1–10. [[CrossRef](#)]
13. Corbett, G.T.; Gonzalez, F.J.; Pahan, K. Activation of peroxisome proliferator-activated receptor α stimulates ADAM10-mediated proteolysis of APP. *Proc. Natl. Acad. Sci.* **2015**, *112*, 8445–8450. [[CrossRef](#)] [[PubMed](#)]
14. Husson, M.; Enderlin, V.; Delacourte, A.; Ghenimi, N.; Alfos, S.; Pallet, V.; Higuieret, P. Retinoic acid normalizes nuclear receptor mediated hypo-expression of proteins involved in β -amyloid deposits in the cerebral cortex of vitamin A deprived rats. *Neurobiol. Dis.* **2006**, *23*, 1–10. [[CrossRef](#)] [[PubMed](#)]
15. Corcoran, J.P.T.; So, P.L.; Maden, M. Disruption of the retinoid signalling pathway causes a deposition of amyloid beta in the adult rat brain. *Eur. J. Neurosci.* **2004**, *20*, 896–902. [[CrossRef](#)] [[PubMed](#)]
16. D'Aniello, E.; Fellous, T.; Iannotti, F.A.; Gentile, A.; Allarà, M.; Balestrieri, F.; Gray, R.; Amodeo, P.; Vitale, R.M.; Di Marzo, V. Identification and characterization of phytocannabinoids as novel dual PPAR α/γ agonists by a computational and in vitro experimental approach. *Biochim. Biophys. Acta Gen. Subj.* **2019**, *1863*, 586–597. [[CrossRef](#)]
17. Vitale, R.; D'Aniello, E.; Gorbi, S.; Martella, A.; Silvestri, C.; Giuliani, M.; Fellous, T.; Gentile, A.; Carbone, M.; Cutignano, A.; et al. Fishing for Targets of Alien Metabolites: A Novel Peroxisome Proliferator-Activated Receptor (PPAR) Agonist from a Marine Pest. *Mar. Drugs* **2018**, *16*, 431. [[CrossRef](#)]
18. Vitale, R.M.; Rispoli, V.; Desiderio, D.; Sgammato, R.; Thellung, S.; Canale, C.; Vassalli, M.; Carbone, M.; Ciavatta, M.L.; Mollo, E.; et al. In Silico identification and experimental validation of novel anti-alzheimer's multitargeted ligands from a marine source featuring a "2-aminoimidazole plus aromatic group" scaffold. *ACS Chem. Neurosci.* **2018**, *9*, 1290–1303. [[CrossRef](#)]
19. Vitale, R.M.; Gatti, M.; Carbone, M.; Barbieri, F.; Felicità, V.; Gavagnin, M.; Florio, T.; Amodeo, P. Minimalist Hybrid Ligand/Receptor-Based Pharmacophore Model for CXCR4 Applied to a Small-Library of Marine Natural Products Led to the Identification of Phidianidine A as a New CXCR4 Ligand Exhibiting Antagonist Activity. *ACS Chem. Biol.* **2013**, *8*, 2762–2770. [[CrossRef](#)]
20. Kashman, Y.; Rotem, M. Muqubilin, a new c24-isoprenoid from a marine sponge. *Tetrahedron Lett.* **1979**, *20*, 1707–1708. [[CrossRef](#)]
21. Sperry, S.; Valeriote, F.A.; Corbett, T.H.; Crews, P. Isolation and cytotoxic evaluation of marine sponge-derived norterpene peroxides. *J. Nat. Prod.* **1998**, *61*, 241–247. [[CrossRef](#)] [[PubMed](#)]
22. Lefranc, F.; Nuzzo, G.; Hamdy, N.A.; Fakhr, I.; Moreno Y Banuls, L.; Van Goietsenoven, G.; Villani, G.; Mathieu, V.; van Soest, R.; Kiss, R.; et al. In vitro pharmacological and toxicological effects of norterpene peroxides isolated from the red sea sponge *Diacarnus erythraeanus* on normal and cancer cells. *J. Nat. Prod.* **2013**, *76*, 1541–1547. [[CrossRef](#)] [[PubMed](#)]
23. Chao, C.-H.; Chou, K.-J.; Wang, G.-H.; Wu, Y.-C.; Wang, L.-H.; Chen, J.-P.; Sheu, J.-H.; Sung, P.-J. Norterpene peroxides and related peroxides from the formosan marine sponge *negombata corticata*. *J. Nat. Prod.* **2010**, *73*, 1538–1543. [[CrossRef](#)] [[PubMed](#)]
24. Ibrahim, S.R.M.; Ebel, R.; Wray, V.; Müller, W.E.G.; Edrada-Ebel, R.; Proksch, P. Diacarpoxides, norterpene cyclic peroxides from the sponge *diacarnus megaspinorhabdosa*. *J. Nat. Prod.* **2008**, *71*, 1358–1364. [[CrossRef](#)] [[PubMed](#)]

25. Qi, J.S.; Desai-Yajnik, V.; Greene, M.E.; Raaka, B.M.; Samuels, H.H. The ligand-binding domains of the thyroid hormone/retinoid receptor gene subfamily function in vivo to mediate heterodimerization, gene silencing, and transactivation. *Mol. Cell. Biol.* **1995**, *15*, 1817–1825. [[CrossRef](#)] [[PubMed](#)]
26. Cesario, R.M.; Stone, J.; Yen, W.-C.; Bissonnette, R.P.; Lamph, W.W. Differentiation and growth inhibition mediated via the RXR:PPAR γ heterodimer in colon cancer. *Cancer Lett.* **2006**, *240*, 225–233. [[CrossRef](#)] [[PubMed](#)]
27. Abba, M.C.; Hu, Y.; Levy, C.C.; Gaddis, S.; Kittrell, F.S.; Zhang, Y.; Hill, J.; Bissonnette, R.P.; Medina, D.; Brown, P.H.; et al. Transcriptomic signature of Bexarotene (Retinoid LGD1069) on mammary gland from three transgenic mouse mammary cancer models. *BMC Med. Genom.* **2008**, *1*, 40. [[CrossRef](#)] [[PubMed](#)]
28. D’Aniello, E.; Rydeen, A.B.; Anderson, J.L.; Mandal, A.; Waxman, J.S. Depletion of retinoic acid receptors initiates a novel positive feedback mechanism that promotes teratogenic increases in retinoic acid. *PLoS Genet.* **2013**, *9*, e1003689. [[CrossRef](#)]
29. D’Aniello, E.; Ravisankar, P.; Waxman, J.S. Rdh10a provides a conserved critical step in the synthesis of retinoic acid during zebrafish embryogenesis. *PLoS ONE* **2015**, *10*, e0138588. [[CrossRef](#)]
30. Mandal, A.; Rydeen, A.; Anderson, J.; Sorrell, M.R.J.; Zygmunt, T.; Torres-Vázquez, J.; Waxman, J.S. Transgenic retinoic acid sensor lines in zebrafish indicate regions of available embryonic retinoic acid. *Dev. Dyn.* **2013**, *242*, 989–1000. [[CrossRef](#)]
31. Waxman, J.S.; Yelon, D. Zebrafish retinoic acid receptors function as context-dependent transcriptional activators. *Dev. Biol.* **2011**, *352*, 128–140. [[CrossRef](#)] [[PubMed](#)]
32. Yang, F.; Wang, R.-P.; Xu, B.; Yu, H.-B.; Ma, G.-Y.; Wang, G.-F.; Dai, S.-W.; Zhang, W.; Jiao, W.-H.; Song, S.-J.; et al. New antimalarial norterpene cyclic peroxides from Xisha Islands sponge *Diacarnus megaspinorhabdosa*. *Bioorg. Med. Chem. Lett.* **2016**, *26*, 2084–2087. [[CrossRef](#)] [[PubMed](#)]
33. Hassinen, T.; Peräkylä, M. New energy terms for reduced protein models implemented in an Off-Lattice force field. *J. Comput. Chem.* **2001**, *22*, 1229–1242. [[CrossRef](#)]
34. Clark, M.; Cramer, R.D.; Van Opdenbosch, N. Validation of the general purpose tripos 5.2 force field. *J. Comput. Chem.* **1989**, *10*, 982–1012. [[CrossRef](#)]
35. Marenich, A.V.; Cramer, C.J.; Truhlar, D.G. Universal solvation model based on solute electron density and on a continuum model of the solvent defined by the bulk dielectric constant and atomic surface tensions. *J. Phys. Chem. B* **2009**, *113*, 6378–6396. [[CrossRef](#)] [[PubMed](#)]
36. Fox, T.; Kollman, P.A. Application of the RESP Methodology in the Parametrization of Organic Solvents. *J. Phys. Chem. B* **1998**, *102*, 8070–8079. [[CrossRef](#)]
37. Trott, O.; Olson, A.J. Software news and update AutoDock Vina: Improving the speed and accuracy of docking with a new scoring function, efficient optimization, and multithreading. *J. Comput. Chem.* **2010**, *31*, 455–461.
38. Morris, G.M.; Huey, R.; Lindstrom, W.; Sanner, M.F.; Belew, R.K.; Goodsell, D.S.; Olson, A.J. AutoDock4 and AutoDockTools4: Automated docking with selective receptor flexibility. *J. Comput. Chem.* **2009**, *30*, 2785–2791. [[CrossRef](#)]
39. Götz, A.W.; Williamson, M.J.; Xu, D.; Poole, D.; Le Grand, S.; Walker, R.C. Routine Microsecond Molecular Dynamics Simulations with AMBER on GPUs. 1. Generalized Born. *J. Chem. Theory Comput.* **2012**, *8*, 1542–1555. [[CrossRef](#)]
40. Wang, J.; Wolf, R.M.; Caldwell, J.W.; Kollman, P.A.; Case, D.A. Development and testing of a general amber force field. *J. Comput. Chem.* **2004**, *25*, 1157–1174. [[CrossRef](#)]
41. Ryckaert, J.-P.; Ciccotti, G.; Berendsen, H.J.C. Numerical integration of the cartesian equations of motion of a system with constraints: molecular dynamics of n-alkanes. *J. Comput. Phys.* **1977**, *23*, 327–341. [[CrossRef](#)]
42. Pettersen, E.F.; Goddard, T.D.; Huang, C.C.; Couch, G.S.; Greenblatt, D.M.; Meng, E.C.; Ferrin, T.E. UCSF Chimera—A visualization system for exploratory research and analysis. *J. Comput. Chem.* **2004**, *25*, 1605–1612. [[CrossRef](#)] [[PubMed](#)]
43. Iannotti, F.A.; Panza, E.; Barrese, V.; Viggiano, D.; Soldovieri, M.V.; Tagliatela, M. Expression, localization, and pharmacological role of kv7 potassium channels in skeletal muscle proliferation, differentiation, and survival after myotoxic insults. *J. Pharmacol. Exp. Ther.* **2010**, *332*, 811–820. [[CrossRef](#)] [[PubMed](#)]

